Photophysical study of assembles between GQDs-Porphyrin as potentials Donor-Acceptor couples for FRET-based biosensors of bacteria

AUTHOR:

Wendy Camila ANZOLA MUNOZ

Supervisors:

Dr. Hafsa KORRI-YOUSSOUFI

Pf. Rachel MEALLET

M2 Internship SERP+ EMJMD program, Université Paris-Saclay

2024

This page has been intentionally left blank

Table of Contents

Acknowledgments 4
Abstract 5
Résumé 5
List of Abbreviations 6
1 Introduction 7
1.1 Photophysical theory 7
1.1.1 FRET applications 8
1.2 GQD as donors 8
1.2.1 photophysical properties 8
1.3 Porphyrins as acceptor 9
1.4 GQDs-porphyrin couple studies in FRET phenomenon 10
2 Scope of the work 11
3 Materials, equipment, and methods 12
3.1 Materials and Equipment 12
3.2 Methods 13
3.2.1 Hydrothermal Synthesis of Graphene Quantum Dots 13
3.2.2 Solvothermal Synthesis of Graphene Quantum Dots 13
3.2.3 Formation of nanocomposites 14
4 Results and discussion 16
4.1 Graphene quantum dots synthesis 16
4.1.1 Characterization of GQD-EDAt 16
4.1.2 Photophysical properties 17
4.2 Porphyrins 18
4.3 Preliminary studies of GQDs and porphyrins 20
4.3.1 Effect of the solvent in GQDs photophysical properties 20
4.3.2 Effect of the solvent in porphyrins photophysical properties 21
4.4 Study of GQDs-Porphyrin assemblies 22
5 Conclusions 26
6 Future perspectives 26
7 Bibliography 27

Acknowledgments

I would like to express my most sincere gratitude to my supervisors Dr Hafsa KORRI-YOUSSOUFI and Pf. Rachel MEALLET for their unwavering patience, kindness and consideration throughout this project. Their guidance and support, always present to assist and encourage me in the hardest moments, were my motivation. I appreciate deeply their confidence in me, allowing me to explore and have space of discussion. I also would like to thank Pf Hélene DORIZON, for her invaluable presence, willing to exchange ideas.

I extend my sincere gratitude to every team member at ICMMO (Institut de Chimie Moléculaire et des Matériaux d'Orsay), ISMO (Institut des Sciences Moléculaires d'Orsay), t. To the Université Paris-Saclay and CNRS for the funding of this project.

I express my heartfelt gratitude to Riccardo Ossanna (PhD student at ISMO) for his unconditional support, willingness to encourage and develop my critical thinking. To every member at ISMO, especially Fabian Dorado and Mariah Harris, for their presence and help.

I am extremely grateful to the European Commission and the SERP+ program for giving me the opportunity to have outstanding education surrounded by incredible people. To the wonderful friends I met in SERP+, that supported me in every country and during these beautiful two years. You were the most amazing part of this experience, and I will be always grateful for the happiness you brough to my life.

Finally, I extend my gratitude to my family for her education, support and love, in every decision I have made.

Abstract

Bacteria detection is an important activity in relevant sectors such as health, food industry and quality control. Fast, accurate, and versatile mechanisms of detection are required for the increase in demand. FRET (Förster Resonance Energy Transfer) occurs usually through the detection of energy transfer between a donor and an acceptor interacting at distances between 1 to 10 nm. FRET can be used to detect bacteria. This study investigates the formation of nanocomposites and the occurrence of FRET between graphene quantum dots (GQDs) functionalized with ethylenediamine (EDA) acting as donors (D) and four different porphyrins: $H_2TPP(OH)_4$, $ZnTPP(OH)_4$, H_2TMPyP, and ZnTMPyP acting as acceptors (A). A set of solutions for each couple D-A was prepared varying ratios of mmol of porphyrin per gram GQDs maintaining a constant GQDs concentration while increasing porphyrin concentration. Absorption and emission spectra were recorded for each sample and were used to decipher photo physics by exciting the donor GQDs at their maximum absorption (350 nm). Three of the proposed D-A couples presented quenching of the donor after addition of acceptor. Evidence of FRET is not as straightforward as envisioned. The presence of a different mechanism is likely to occur (such a phenomenon could not be investigated due to lack of time).

Résumé

La détection des bactéries est une activité importante dans des secteurs tels que la santé, l'industrie alimentaire et le contrôle qualité. Des mécanismes de détection rapides, précis et polyvalents sont nécessaires pour répondre à la demande croissante. Le FRET (transfert d'énergie par résonance de Förster) est un phénomène photophysique entre un donneur et un accepteur interagissant à des distances comprises entre 1 et 10 nm. Le FRET peut être un moyen de détecter des bactéries. Cette étude examine la formation de nanocomposites et la présence (ou l'absence) de FRET entre des boîtes quantiques de graphène (GQDs) fonctionnalisées avec de l'éthylènediamine (EDA) agissant comme donneurs (D) et quatre porphyrines différentes : $H_2TPP(OH)_4$, $ZnTPP(OH)_4$, H_2TMPyP, et ZnTMPyP agissant comme accepteurs (A). Un ensemble de solutions pour chaque couple D-A a été préparé en faisant varier les rapports de mmol de porphyrine par gramme de GQDs, en maintenant une concentration constante de GQDs tout en augmentant la concentration de porphyrine. Les spectres d'absorption et d'émission ont été enregistrés pour chaque échantillon, et ont permis d'étudier la photophysique des systèmes, en excitant les GQDs (donneurs) à leur absorption maximale (350 nm). Trois des couples D-A proposés ont présenté une extinction de la luminescence du donneur (quenching) après addition de l'accepteur. Il n'y a pas de preuve claire de FRET, les résultats suggèrent la présence d'un autre mécanisme d'extinction (qui n'a pas pu être investigué par manque de temps).

List of Abbreviations

AIE aggregation-induced emission

D-A Donor-acceptor

DMSO Dimethyl sulfoxide

EDA Ethylenediamine

FRET Förster resonance energy transfer

FTIR Fourier-transform infrared spectroscopy

GQDs Graphene quantum dots

H_2TMPyP 5, 10, 15, 20-(tetra-N-methyl-4-pyridyl)porphyrin tetrachloride

H_2TPP(OH)$_4$ Tetrakis(para-hydroxyphenyl)porphyrin

ICT intramolecular charge transfer

PET photo-induced electron transfer

PL Photoluminescence

QCE quantum confinement effects

SSE surface state effects

TCSPC time-correlated single photon counting

TEM Transmission electron microscopy

TMPyP Tetramethylpyridinio

TPP Tetraphenylphorphyrin

UV Ultra-Violet

ZnTMPyP Zinc(II) 5, 10, 15, 20-(tetra-N-methyl-4-pyridyl)porphyrin tetrachloride

ZnTPP zinc(II)tetrakis(4-phenyl)porphyrin

ZnTPP(OH)4 Zinc(II) tetrakis(para-hydroxyphenyl)porphyrin

ZP Zeta Potential

1 Introduction

Detection of pathogenic bacteria is a crucial activity in many economically relevant sectors such as the food, the medical industry, or for quality control. Real-time and continuous detection mechanisms are increasingly necessary, requiring versatile systems that can adapt to different environments. The drawbacks in detection limits, specificity, accuracy and prices represent an obstacle to adapting the technique to different problems[1]. Thus, the development of versatile detection methods is necessary.

The scientific community research innovative mechanisms to tackle the problem. One line of research aims to employ biosensors as detectors. This system works by detecting a signal generated after the interaction between the target object and the bioreceptor. There are several detection methods: electrical, optical, thermal, or mass-based. [2]

Optical biosensors can take advantage of multiple mechanisms for signal detection, such as surface plasmon resonance (SPR), ring resonator, fluorescence/luminesce, and others. In an optical fluorescence biosensor, light out from a fluorescence process is detected with a photodiode or a photomultiplier.[2] This category of biosensors is interesting for its promising application in the detection of low-concentrated samples and systems with complex matrices[3]. In addition, their versatility makes them a promising technology adaptable to different needs.

1.1 Photophysical Theory

Förster resonance energy transfer (FRET) is a photo-physicochemical and non-radiative process occurring after the interaction of the electronic excited states of two molecules. A donor molecule is excited to the first excited singlet state (S_1) through the absorption of light. This can return to the ground state (S_0) followed by fluorescence, or through FRET, where it can transfer its energy to an acceptor molecule in its ground state (S_0). The transferred energy allows the acceptor to be excited to the first excited singlet state (S_1). After the transfer, the donor molecule returns to the ground state (S_0) without emitting fluorescence[4]. The acceptor molecule then returns to the ground state (S_0) by emission of fluorescence or by non-radiative relaxation. The mechanism can be observed in **Figure 1**, in a Jablonski diagram.

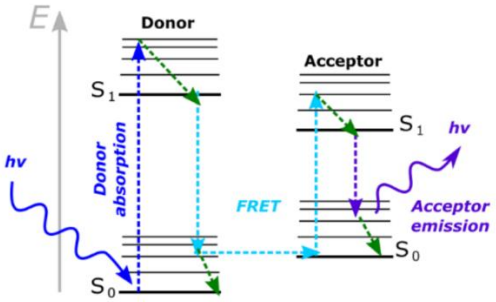

Figure 1 Jablonski diagram for FRET (in that case acceptor is luminescent)[5]

Three requirements must be met for FRET to occur. First, FRET requires the donor and acceptor to be within 1 to 10 nm of each other as the energy transfer efficiency between the donor and acceptor molecules decreases with the sixth power of the distance that separates them[4]. Second, the absorption band of the acceptor must overlap the fluorescence emission band of the donor (**Figure 2**) and third, the donor's lifetime must be sufficiently long[4]. Finally, the relative orientation of transient dipole moments of the donor and acceptor (if they are perpendicular, the FRET probability is zero). This particular energy transfer manifests as a quenching in the

donor's emission of fluorescence and an enhancement in the fluorescence of the acceptor[6], whenever the acceptor is an emissive species.

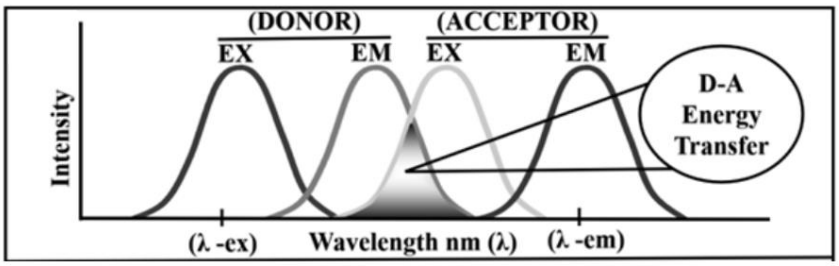

Figure 2 Spectral overlap between donor and acceptor[6]

1.1.1 FRET Applications

The importance of FRET in sensing lies in the fact that the distance between the donor and acceptor can be readily influenced by the presence of biomolecules, metals, or other species that interact with either the donor or acceptor[6]. This makes FRET particularly valuable for monitoring conformational changes when the donor and acceptor are labeled with target molecules. Consequently, FRET is highly useful for observing cellular events and interactions within biological systems both *in vivo* and *in vitro*. FRET-based biosensors exhibit high specificity, allowing them to detect specific biomolecules or environmental changes without interference from other factors[6]. Their sensitivity and versatility make them useful in various environments, as will be explained.

FRET is valuable for its ability to assess both intermolecular and intramolecular interactions, as well as to track enzyme kinetics. Indeed, it has been employed in the development of immunosensors to detect reactions between antigens and antibodies[6]. Single-molecule detection level can be achieved, allowing the detection of exceptionally low concentrations of small molecules like metals[7], drugs, and food additives. FRET can be used to monitor enzymatic biosensor. In this application, a reaction is followed by a FRET-labeled substrate catalyzing the conversion of the substrate into a product. FRET-aptasensors employ donors or acceptors labeled with short oligonucleotides or peptides, specifically chosen for their high affinity to targets via ssRNA/ssDNA selection. These sensors are characterized by exceptional selectivity, stability, and affinity, along with their non-toxic nature.[6]

The versatility of a FRET-based biosensor hinges on the limitless combinations possible between donors and acceptors. Challenges in employing FRET for sensing lie in the precise matching of donor-acceptor pairs to ensure optimal energy transfer under specified conditions[6].

1.2 GQD As Donors

1.2.1 Photophysical Properties

Fluorophores like fluorescent nanoparticles, nanoclusters, and polymers are investigated in FRET sensors due to their photoluminescent (PL) characteristics. Quantum dots are particularly intriguing for FRET research due to their ability to serve as both donors and acceptors. They are noted for their high luminescence quantum yields, reported as high as 99% in the literature, broad-band absorption capabilities, and resistance to photo-bleaching[9].

Graphene quantum dots (GQDs) are nanomaterials consisting of a monolayer or a few layers of graphene. They are notable because of their low toxicity, solubility, luminous emission, biocompatibility, and high surface area.[10] These materials are smaller than 10 nm, which allows them to experience quantum confinement effects (QCE) and surface state effects (SSE)[10]. QCE

is the change in optical and electronic properties due to particle size and π-domains insulated on the graphene planes. SSE refers to the effect of the surface configuration by doping the edge with functional groups. This means that they have a precise structure-property and a strong-size dependent relationship that can be controlled and influenced by the synthetic method.[11]

In UV-vis spectroscopy GQDs show an absorption band located in the range of 350~600 nm attributed to the electron transitions of the surface functional groups as carboxylic acid, and alcohol, among others depending on the route of the synthesis. The absorption band maxima located in the region of 280~350 nm is attributed to electronic transitions from C=O or C–O bonds to π-π*.[12] Concerning emission, it tipically stems from surface/edge state and conjugated π-domains.[10] In steady-state fluorescence spectroscopy, the emission band is found between 400 and 700 nm, according to their size. There is a linear correlation between emission wavelength and size, with larger quantum dots exhibiting emissions that are red-shifted. (**Figure 3**)[11].

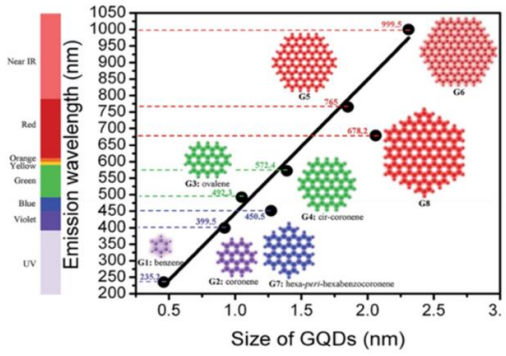

Figure 3 Size dependance of PL properties in GQDs[12]

1.2.2 Synthesis

GQD can be synthesized by top-down and bottom-up approaches. Top-down approaches refer to the use of bulk carbon nanomaterials such as carbon nanotube fullerene or graphene that are broken down into "monomers", smaller structures. The following are examples of synthetic techniques that employ a top-down approach: chemical exfoliation, laser ablation, ultrasonic-assisted treatment and etching[9].

The bottom-up approach consists of the synthesis of GQDs from small molecule precursors and by heating it can form carbonized structures depending on the synthesis precursor and the conditions the structures of GQDs could be controlled. Popular bottom-up synthetic methods are microwave synthesis, solvothermal, and hydrothermal. Solvothermal and hydrothermal synthesis are interesting because they are considered fast synthesis protocols, and they require cheap equipment and materials in comparison with other mentioned techniques.

Furthermore, surface configuration can be altered post-synthesis to achieve different electronic properties. There are several approaches available, including the incorporation of modified precursors to introduce heteroatom doping[12].

1.3 Porphyrins As Acceptors

Porphyrins are macrocycles characterized by cyclized pyrroles. In Porphyrins, four pyrroles are connected through methylidene bridges (*meso*), forming a ring. This porphyrinic ring has a square rigid planar core with an extended conjugated π-electron system, capable of coordinating with metals such as *Zn(II) or Fe(III),* among others. Porphyrins are highly versatile compounds

because their chemical and electronical properties can be tuned with ease by functionalization of the meso- or the β-position, or even their metal center (**Figure 4)**. Porphyrins are also known for their tendency to aggregate. Ionic strength, solvent polarity, pH, and other factors can influence the state of aggregation and lead to the formation of type-J- and H aggregates.[16]

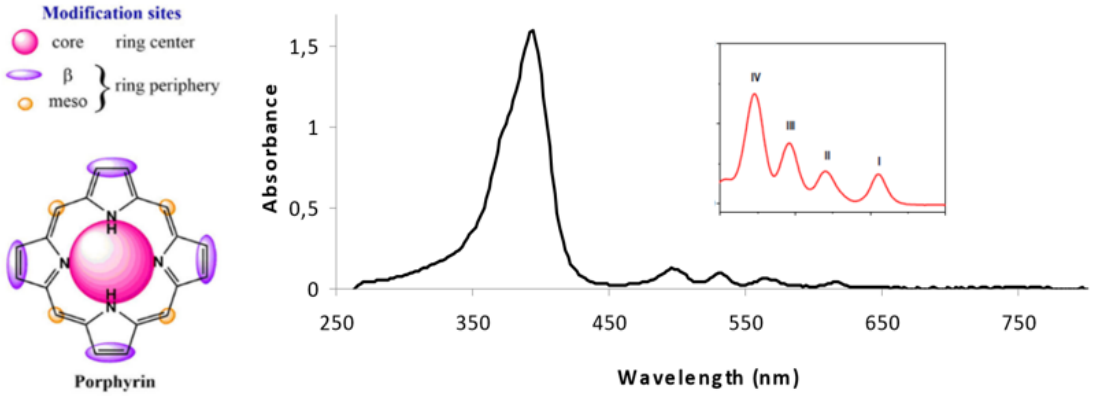

Figure 4 Modification sites in porphyrins and example of the shape of an absorption spectrum in free-core porphyrins.

1.3.1 Photophysical properties

Due to their highly conjugated π-electron system, porphyrins absorb light in the visible range and display a distinct spectrum characterized by an intense π-π* transition band, the Soret band, accompanied by four other bands, the Q-bands. The Soret band typically occurs between 410 and 450 nm in wavelength. This band corresponds to the transition from S_o while Q-bands between 600 and 800 nm. The Q bands are usually sensitive to S_3 and S_4. Q-bands provide information on macrocycle substitution and the nature of the fixed metal ion to the core. For metalated porphyrins, the number Q bands is reduced from four to just two, corresponding to transitions from the ground state S_o to the first S_1 and second S_2 excited state. This can be explained as the results of an increase in symmetry, going from a D_{2h} to a D_{4h} structure[14]. Q bands provide information about the geometry of the metal-center: As an example, a stable, square-planar complex is evidenced by the first Q band being higher than the second[15]. When exciting the Soret band, the emission of fluorescence is characterized by intense bands between 600 and 800 nm. The complexation of metal ions induces a blue shift of the emission, with respect to their free-core counterpart.

1.3.2 Coupling of GQDs and Porphyrins

Some studies have reported FRET phenomenon made of GQDs as donors and porphyrin structures as acceptors. The arrangement between the couple is called nano ensembles, composites or nanocomposites and Some examples will be addressed.

Authors have studied FRET phenomenon between tetrakis(m-nitrophenyl) porphyrin and GQDs by a solvothermal method using citric acid as a carbon source, for singlet oxygen generation. They characterized the energy transfer through emission and absorption spectroscopy with complementary studies with TCSPC.[30]

Recent researchers have developed FRET-based sensors for Fe(II) detection between meso-tetra(4-sulfonatophenyl) porphyrin (TSPP) and oil soluble GQDs. The reliability was evaluated in biological matrices such a fetal bovine serum and muscle tissue homogenate.[7]

There are reports of the formation of nanocomposites between GQDs made from graphene oxide and Tetrasodium-meso-tetra(4-sulfonate phenyl) porphyrin dodecahydrate (NaTSPP), and the presence of FRET-confirmed through absorption and emission spectroscopy.[17]

Biosensors for biothiols have been studied through probe design between maleimide functionalized GQDs and tetrakis (4-aminophenyl) porphyrin (TAPP) interacting through FRET. They report successful results in the detection of biothiol using the system proposed with a detection range between $6.7x10^{-10}$ to $2x10^{-7}$ mol/L and a detection limit of $2.3x10^{-10}$ mol/L.[18]

Regarding similar systems, some authors have studied π-π stacking between porphyrin and graphene oxide (GO). They reported the isolation of the hybrid materials and characterization through FTIR, XPS, Raman spectroscopy, and SEM.[19]

Previous studies provide fundamental insights into the study of the formation of nanocomposites between the proposed GQDs and porphyrin structures to form D(donor)-A(acceptor) couple for FRET. As an innovation, our approach consists of the generation of nanocomposites with potential use in bacteria detection.

2 Scope of the work

The goal of the project is to develop efficient nanocomposites through non-covalent interaction, specifically through π-π stacking, between GQDs and some tetraphenyl porphyrins (TPP), and to study the presence or absence of FRET through absorption and emission spectroscopy. The interest of the nanocomposites is for future applications in the design of bacteria biosensors through the mechanism proposed in **Scheme 1**.

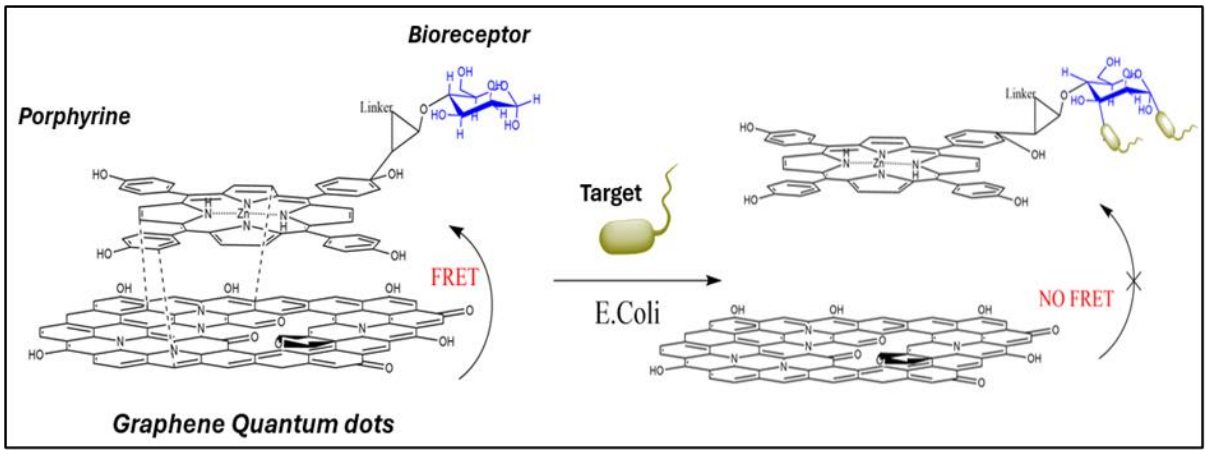

Scheme 1 Proposal of working mechanism of a biosensor based on FRET. GQDs acting as donors interact through π-π stacking (dashed lines) with an acceptor (porphyrin) sugar-labeled (bioreceptor).

To achieve this goal, GQDs will be obtained by two methods: solvothermal and hydrothermal synthesis, with an *N*-dopping approach to evaluate their effect on their photophysical properties. In addition, different types of porphyrins will be tested to evaluate the effect of their chemical structure and solubility on their capability to interact with GQDs (**Figure 5**).

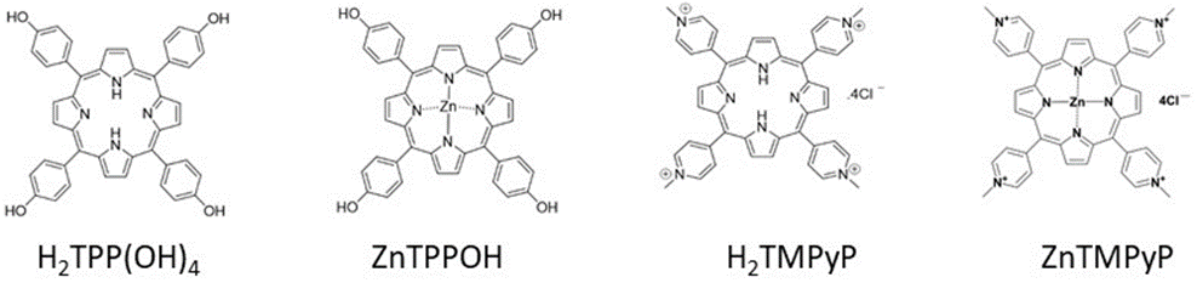

Figure 5: Chemical structures of proposed porphyrins for the formation of nanocomposites

The chemical structure study will be done through comparison based on its charge, for effects in association-dissociation processes and the addition of zinc effect in the photophysical process.

Moreover porphyrin can be easily modified through the attachment of biomarkers such as polymeric structures, that can act as bioreceptors in the design of biosensors. The described D-A system was selected due to its supposedly favorable conditions that should increase the chances of observing FRET. The enriched π-domains present in both structures, GQDs and porphyrin, are likely to support a high π-π stacking interaction (proximity of donor and acceptor).

In addition, the system fulfills other FRET conditions, mentioned as follows:

- Overlapping absorption band of the porphyrins (acceptors) located between 420 and 440 nm, and the emission band of GQD (donor) around 440 nm.
- Enriched electron-density regions in GQD and porphyrin structure that could favor the formation of π-π stacking
- High Planarity in porphyrins and GQDs structure that could affect relative dipole interaction.
- No overlap of emission bands of porphyrin with the emission band of GQDs, so porphyrin will not hide the donor signal in case there is the presence of FRET.

3 Materials, equipment, and methods

3.1 Materials and Equipment

EDA: Ethylenediamine, Citric acid, Dimethylsulfoxide (DMSO) provided by Sigma Aldrich, DMF: N-N dimethylformamide from Carlo Erba reagents S.A.S. Porphyrin $H_2TPP(OH)_4$. MW: 678 g/mol tetrakis(*para*-hydroxyphenyl)porphyrin, and H_2TMPyP 5, 10, 15, 20-(tetra-*N*-methyl-4-pyridyl)porphyrin tetrachloride, MW: 795,8 g/mol , are synthesized in the laboratory ICMMO. ZnTMPyP (Zinc(II) 5, 10, 15, 20-(tetra-*N*-methyl-4-pyridyl)porphyrin tetrachloride). CAS 28850-44-4, MW: 884.01 g/mol are provided by Porphychem and $ZnTPP(OH)_4$ (Zinc (II) tetrakis(*para*-hydroxyphenyl)porphyrin), synthesized in the laboratory from $H_2TPP(OH)_4$, characterized through NMR and absorption spectroscopy. MW: 741.33 g/mol

Equipment

UV-visible spectra were recorded on a UV-2600 UV-VIS Spectrometer by Shimadzu Scientific Instruments. Measurements were done in a quartz cuvette. ***Dynamic light scattering (DLS) and Z-Potential*** measured in a ZEN 3600 by Malvern Panalytical. Disposable cuvette DTS0012 was used for DLS measurements and a disposable folded capillary cell DTS1070 was used for zeta measurements. Solutions were prepared before each measurement controlling pH and

concentration. ***Freeze dryer*** Lyovapor L-200/L-200 Pro by BUCHI ***Fluorescence spectroscopy*** was conducted with a FluoroMax-plus Spectrofluorometer (Horiba Jobin-Yvon). Spectra are corrected from apparatus response function (IRF) and lamp fluctuations. Measurement was done in a quartz cuvette. ***Luminescence quantum yield*** measurements were measured with a 100 mm diameter Spectralon integrating sphere unit (Shimadzu) on a SHIMADZU Fluorescence Spectrofluorometer RF-6000.

3.2 Methods

3.2.1 Hydrothermal Synthesis of Graphene Quantum Dots

(The synthesis was performed with the hydrothermal method described in the literature[20] with small modification)

Synthesis of GQD-EDAt: Citric acid (0.21 g, 1 mmol) and ethylenediamine (EDA, 0.18 g, 3 mmol) were dissolved in 5 mL of water and stirred until complete solubility. Then the solution was transferred to a 20 mL autoclave, which was then sealed and heated to 160 °C in an electric oven for 4 hours. The reaction mixture was precipitated by adding ethanol, followed by centrifugation at 5000 rpm for 15 minutes. The resulting dark solid was separated from the supernatant and lyophilized for 24 hours to yield a yellowish solid. The solid was dissolved in water, filtered three times through a 0.22 µm filter, and stored at 4 °C. Characterization was conducted after a minimum of 3 days in refrigeration to ensure particle stabilization.

Synthesis of GQD-NaOHt: Citric acid (0.21 g, 1 mmol) and sodium hydroxide (NaOH, 0.12 g, 3 mmol) were dissolved in 5 mL of water. The solution was transferred to a 20 mL autoclave, which was then sealed and heated to 160 °C in an electric oven for 4 hours. The resulting product was processed using the same protocol as for GQD-EDAt.

3.2.2 Solvothermal Synthesis of Graphene Quantum Dots

The synthesis was performed with the protocol reported in literature[18]

Synthesis of GQD-EDAm[21] Citric acid (5 g) was placed in a three-neck round-bottom flask and heated with agitation at 160 °C for 40 minutes until an orange-yellowish product formed. The reaction was then halted, and 15 mL of 2 M ethylenediamine (EDA) was added. The mixture was agitated for 1 hour (pH=10). The product was filtered three times through a 0.22 µm filter and lyophilized for 24 hours, yielding an orange-yellowish viscous substance. The product was dissolved in deionized water and stored at 4 °C. 5 grams of citric acid were placed in a three-head round flask on agitation, at 160°C for 40 minutes. The reaction was stopped when an orange yellowish product was formed. Finally, 15 mL of EDA 2M were added. The liquid was kept in agitation for 1 hour. The final pH is 10. Then was filtrated with a 0.22µm filter three times and lyophilization was done for 24 hours obtaining an orange-yellowish viscous product. The amount was determined by the difference in weight between the round-bottom flask in the presence and absence of the product. GQDs were obtained by dissolving them in a known amount of deionized water, recollected with a Pasteur pipet and storage at 4°C.

Synthesis of GQD-NaOHm: Citric acid (5 g) was placed in a three-neck round-bottom flask, agitated, and heated at 160 °C for 40 minutes until an orange-yellowish product formed. Sodium hydroxide (0.1 M) was added dropwise until complete dissolution of the solid. The solution was then transferred to a beaker and diluted with the following addition of NaOH solution up to 75 mL. The final pH of the solution to a final volume of 75 mL, resulting in a pH of 9.0. The product was then filtered, lyophilized, obtained after filtration, and lyophilization to obtain powder stored following the same protocol for GQD-EDAm.

Synthesis of the metalated Porphyrin ZnTPP(OH)$_4$: 100 mg (0,147 mmol) of $H_2TPP(OH)_4$ and 162 mg (0.737 mmol) of $Zn(OAC)_2H_2O$, were solubilized under argon in 26 mL of DMF added to the system under reflux. The reaction was heated for 3 hours at 82°C. The reaction was monitored via TLC with solvent DCM:MeOH in proportion 95:5 respectively. An extraction with water was done to remove DCM. Finally, it was filtered and washed with a mixture of acetone water to remove the excess of metal and precipitated in a rotary evaporator. Yield: 80.7%.

3.2.3 Formation of nanocomposites

Four donors (GQDs-EDAt)-acceptor(porphyrin) couple were studied. Porphyrin is modified with various functional groups alcohol and pyridinium affording various chemical structure for the GQDs interaction. In addition, the effect of Zn as metal in core of macrocycle was studied. Experiments were performed after preliminary studies of the effect of the solvent DMSO/H_2O on the porphyrins and GQDs. Summary of D-A couple named as **system 1**, **2**, **3** and **4** are reported in **table 1**.

System	Donor	Acceptor (Porphyrin)	Solvent system
1	GQDs-EDAt	$H_2TPP(OH)_4$	DMSO/ H_2O
2	GQDs-EDAt	$ZnTPP(OH)_4$	DMSO/ H_2O
3	GQDs-EDAt	H_2TMPyP	H_2O
4	GQDs-EDAt	ZnTMPyP	H_2O

Table 1. Summary of the Donor-Acceptor systems that are described in this work.

To measure photophysical properties we work with low concentration of GQD and porphyrin to form the complex where the absorbance should be less than 0.1. For this purpose, the concentration of porphyrin varies from 10^{-8} to 10^{-7} M, and the concentration of GQDs at 0.016 mg/mL.

In the case of $H_2TPP(OH)_4$ and, the porphyrins were dissolved in DMSO and mixed with GQDs solubilized in water. For studying the effect of the concentration of the porphyrin in composite, the ratio between the DMSO and water was kept at 50/50 to not disturb the solubility of both porphyrin and GQDs.

A solution of $H_2TPP(OH)_4$ $2.2x10^{-6}$ mol/L in DMSO was prepared as the mother solution. The mother solution of GQDs-EDAs was 0.12 mg/mL. The dilution is performed in the case at 3 mL amber flask. The experiment placed a constant volume of GQD-EDAt dissolved in H_2O. Then, different increasing volumes of porphyrin dissolved in DMSO were added. 3 mL final volume was reached by adding to all experiments 1100 µL of water to have 1500µL of water in total to maintain a constant proportion solvent of 50:50 DMSO:H_2O in the case of porphyrin $H_2TPP(OH)_4$ and $ZnTPP(OH)_4$.

Samples were placed in sonication for 2 hours, then with agitation for 30 minutes; absorbance and fluorescence spectra were measured. Information on volumes and proportions can be seen in **Table 2**.

System 1: $H_2TPP(OH)_4$ + GQDs-EDAt				Solvent: 50% H_20: 50% DMSO		
Mother solution GQDs:0.12 mg/mL in H_2O				Mother solution $H_2TPP(OH)_4$: 2.2 x 10^{-06} mol/L DMSO		
Exp	µL $H_2TPP(OH)_4$	µL GQDs-EDA	µL of DMSO	[$H_2TPP(OH)_4$] (mol/L)	[GQDs-EDAt] (mg/mL)	mmol $H_2TPP(OH)_4$ / g of GQDs
1	50	400	1450	3.7 x 10^{-08}	0.016	2.3 x 10^{-03}
2	80	400	1420	5.9 x 10^{-08}	0.016	3.6 x 10^{-03}
3	100	400	1400	7.4 x 10^{-08}	0.016	4.5 x 10^{-03}
4	150	400	1350	1.1 x 10^{-07}	0.016	6.8 x 10^{-03}
5	200	400	1300	1.5 x 10^{-07}	0.016	9.1 x 10^{-03}
6	250	400	1250	1.8 x 10^{-07}	0.016	1.1 x 10^{-03}
7	350	400	1150	2.6 x 10^{-07}	0.016	1.6 x 10^{-03}
8	450	400	1050	3.3 x 10^{-07}	0.016	2.1 x 10^{-03}
9	550	400	950	4.1 x 10^{-07}	0.016	2.6 x 10^{-03}

Table 2 volumes of mother solutions of GQDs-EDA and $H_2TPP(OH)_4$ in each nanocomposite. The volume of DMSO added to have a total volume of 1,5 mL. Concentrations of GQDs-EDAt and $H_2TPP(OH)_4$ in the experiment. Ratio mmol of $H_2TPP(OH)_4$ and gram of GQDs-EDAt. Volume of 3 mL was reached adding 1100µL to all the experiments.

Nanocomposites for **system 2**: $ZnTPP(OH)_4$ and GQD-EDAs, were conducted as the previous one. The difference is that the mother solution of $ZnTPP(OH)_4$ was $9x10^{-7}$mol/L, and the volume added was changed to maintain the same order of magnitude of concentration mol/L in the experiments for $H_2TPP(OH)_4$. Conditions of the experiment form by ZnTMPyP and GQDs-EDA are summarized in **table 3**.

System 4 : ZnTMPyP + GQDs-EDAt				Solvent: H_2O	
Mother solution GQDs:0.12 mg/mL			Mother solution ZnTMPyP: 1.7 x 10^{-06} mol/L		
Experiment	µL ZnTMPyP	µL GQDs-EDA	[ZnTMPyP] (mol/L)	[GQDs-EDAt] (mg/mL)	mmol ZnTMPyP / g of GQDs
1	20	400	1.1 x 10^{-08}	0.016	7.0 x 10^{-04}
2	60	400	3.4 x 10^{-08}	0.016	2.1 x 10^{-03}
3	1300	400	7.4 x 10^{-07}	0.016	4.5 x 10^{-02}
4	1000	400	5.7 x 10^{-07}	0.016	3.5 x 10^{-02}
5	1500	400	8.5 x 10^{-07}	0.016	5.2 x 10^{-02}
6	2000	400	1.1 x 10^{-07}	0.016	7.0 x 10^{-02}
7	2600	400	1.5 x 10^{-07}	0.016	9.1 x 10^{-02}

Table 3. Volumes of mother solutions of GQDs-EDA and ZnTMPyP in each sample. Water is added to reach a final volume of 3 mL. Concentrations of GQDs-EDAt and ZnTMPyP in the experiment. Ratio mmol of ZnTMPyP per gram of GQDs-EDA. The final volume of 3 mL was reached with the addition of water.

Briefly, samples were formed with the volumes of GQDs-EDA and *ZnTMPyP* of their respective mother solutions, reported in *Table 3*. The final volume was 3mL, placed in sonication for 2 hours and shaking for 30 minutes. The **experiment for system 3** followed the same protocol used for a system made of *ZnTMPyP*. However, the mother solution of GQDs-EDA was 0.2 mg/mL and $6.4x10^{-06}$ mol/L for the mother solution of H_2TMPyP. The concentration of GQDs in the experiments was 0.026 mg/mL. The concentration of H_2TMPyP was adjusted to have the same order of magnitude as in **Table 3**. After the formation of composites, they were placed in sonication for 2 hours, and then agitation for 30 minutes.

4 Results and discussion

4.1 Graphene quantum dots synthesis

Two synthetical techniques were employed for the synthesis of GQDs. One was found to be more suitable than the other. Methodologies were chosen based on the availability of materials and properties reported in the literature.

Two synthetic methods were employed in the synthesis of GQDs: solvothermal[21] and hydrothermal[20]. Both methods involved pyrolysis, using citric acid as a carbon source. The GQDs structure is written in **scheme 2**.

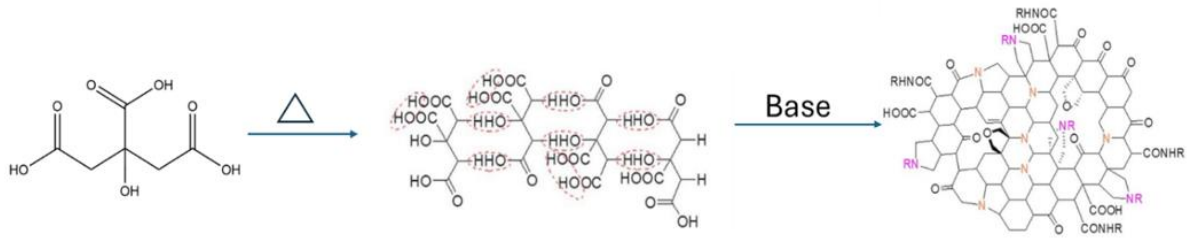

Scheme 2 Formation of graphene quantum dots from pyrolysis of citric acid

The addition of a base allows the start of an aldol condensation and cycloaddition to produce aromatic clusters. The saturation of nucleation allows the formation of GQDs[21]. They were characterized by UV-Visible spectroscopy, fluorescence spectroscopy, TEM, Z-potential, DLS and FT-IR.

The nanoparticles were doped with EDA. The obtained nanoparticles presented maximum absorption around 350 nm, specifically at 346 nm in water with maximum emission at 445 nm with excitation at 350 nm, reported in literature around 450 nm. The luminescence quantum yield turned out to be 47%. In literature is reported values up to 95% through this synthesis method. [20].

4.1.1 Characterization of GQD-EDAt

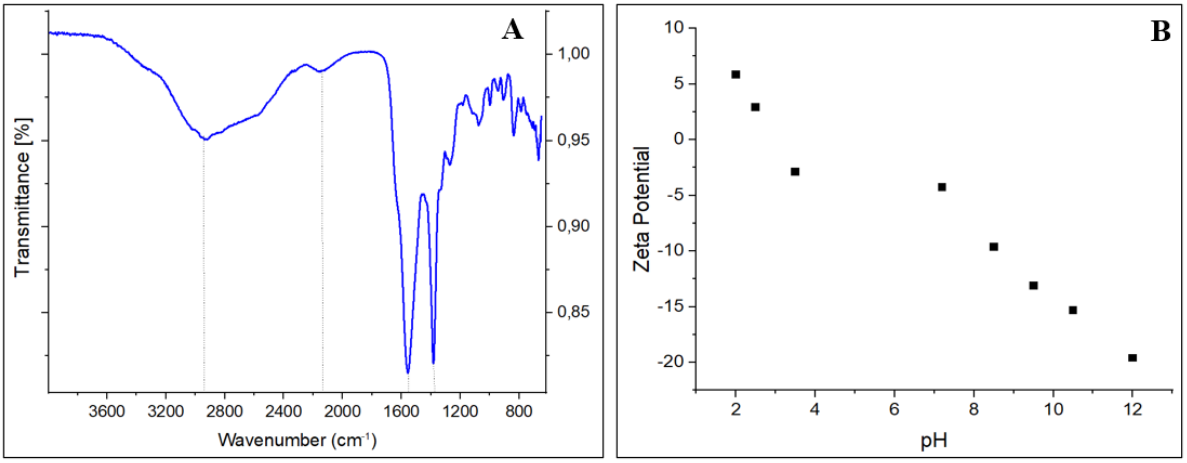

Figure 6. A) FT-IR spectroscopy B) Plot of pH vs Z-potential (ZP)

Functional groups of GQDs were characterized through FT-IR spectroscopy presented in **Figure 6**. A broad band is observed between 2500 and 3200 cm^{-1}. This area is ascribed to the –NH and –OH stretching vibrations. The strong absorption peaks at 1390 and 1570 cm^{-1}

correspond to the symmetric and anti-symmetric stretching vibrations of –COOH respectively, consistent with the expected surface of the carbon dots.[12] In **figure 6 B)** the ZP is positive while below pH 3, however for pH values higher than 3, the ZP decreases, becoming more and more negative as the pH turns more alkaline. This pH-dependance reflects the presence of free, protonable -NH and deprotonable -OH terminal groups. This experiment was done to know the charge of the nanoparticles during the formation of assembles between GQDs and porphyrins.

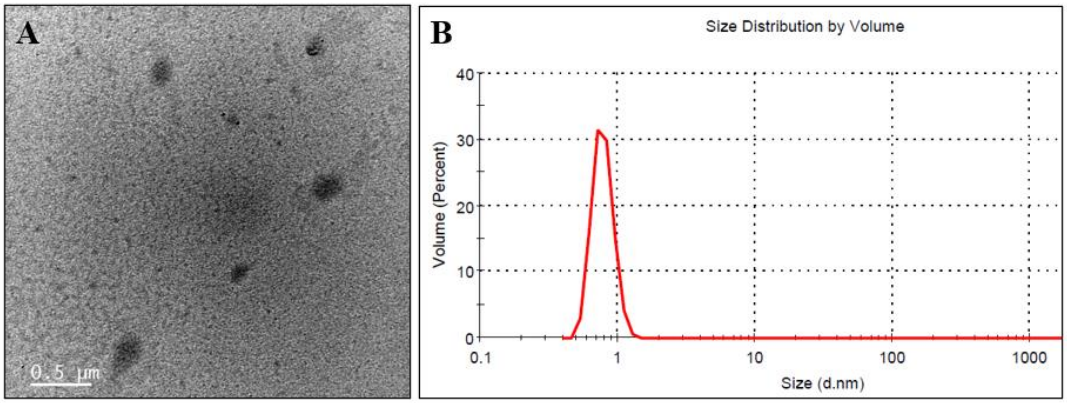

Figure 7 A) TEM representative images. B) Dynamic light scattering results for particle size,

In **Figure 7**, size characterization is presented. TEM images allowed us to observe aggregation of the nanoparticles while DLS measurement allowed us to estimate a particle size of 0.9 nm from the hydrodynamic diameter.

4.1.2 Photophysical properties

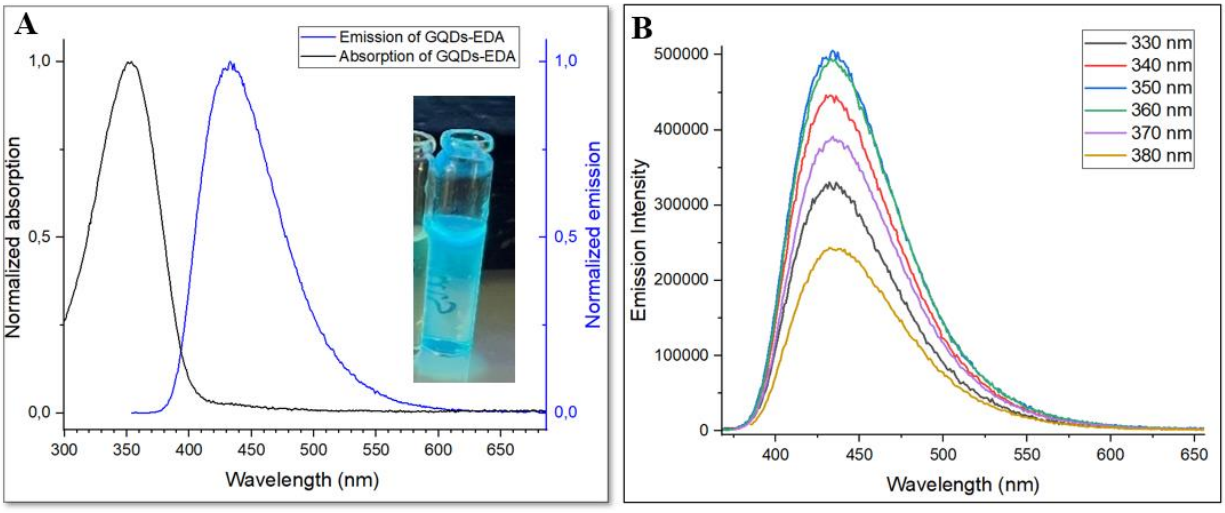

Figure 8 A) Normalized absorption (black) and emission (blue) spectra of GQDs-EDA. GQDs when irradiated with a 270 nm UV lamp. B) Emission spectra of GQDs at different excitation wavelengths from 330 nm up to 380 nm (slit size 1 nm)

GQDs-EDA absorption and emission spectra are shown in **Figure 8**. A broad absorption with maximum absorption at 346 nm in the UV region is assigned to π–π* (C=C) and n–π* (C=O) transitions. For the emission band it is possible to observe a maximum value at 440 nm, and a tail that extends up to 550 nm. In **Figure 8 B)** there is the emission spectrum at different

excitation wavelengths (330 up to 380 nm). Change in the excitation wavelength did not show any shift around the emission band indicating homogeneity over the nature of the GQDs.[18]

A summary of the characterization of GQDs obtained in solvothermal and hydrothermal methods is found in **Table 4**. The results show that the synthesis with the hydrothermal method presents lower particle size and higher luminescence quantum yield in comparison with the solvothermal method. GQD-EDAm has a better quantum yield in comparison with GQD-NaOHm and has a higher particle size. This indicates that the base can affect the properties of GQDs. GQDs with NaOH could not be obtained by the hydrothermal method.

The results allowed us to choose GQD-EDAt as the donors for further experiments

presented *Graphene Quantum dots*	***Particle Size (nm)***	***Z– Potential (mV)***	***Absorption wavelength (nm)***	***Emission wavelength (nm)***	***Luminescence Quantum yield***
GQD-EDAt	0.9	-4.23	346	445	47%
GQD-EDAm	142,50	-26.2	350	440	4.2%
GQD-NaOHm	44,73	-10.3	355	460	1.8 %

Table 4 Summary of physical properties of synthetized graphene quantum dots. *(GQD-XXXy where y stands for (t) hydrothermal method and (m) solvothermal method.)*

The synthesis method influences significantly the characteristics and properties of GQDs-EDA. Despite the same reactants being used, the synthesis with the hydrothermal method presents lower particle size and higher quantum yield. In a hydrothermal reaction, temperature is better controlled because is guaranteed that the system has the same temperature in a determined time. The time of reaction and temperature influence significantly in the properties of GQDs.[20]

The base used for the synthesis also seems to influence their properties. Substitution of carbon atoms for heteroatoms such as nitrogen allows additional electronic states that can favor the PL properties of GQDs.[22] This could explain the high quantum yield values obtained in N-dopped quantum dots in comparison with GQDs formed with NaOH.

4.2 Porphyrins

Porphyrins were characterized by absorption and emission spectroscopy.

Absorption Spectroscopy

Synthesis of $ZnTPP(OH)_4$ was done from $H_2TPP(OH)_4$. The shift of the Soret band from 425 nm is characteristic of $H_2TPP(OH)_4$ to 430 nm and the presence of 2-Q bands in 560 and 605 nm confirms the formation of $ZnTPP(OH)_4$. (**figure 9A**). TMPyPs on the other hand have a shift of 15 nm, due to the presence of pyrydiniumyl groups. (**figure 9B**)

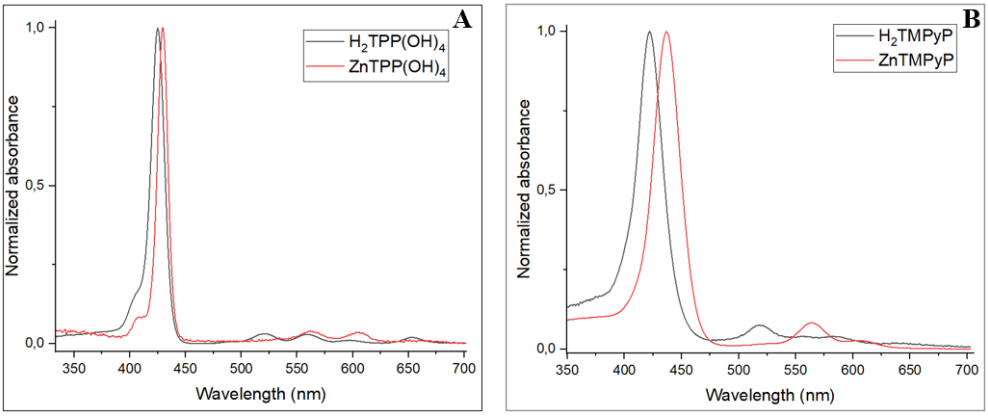

Figure 9 A) Absorption spectra of $H_2TPP(OH)_4$ and $ZnTPP(OH)_4$ in DMSO and B) Absorption spectra of H_2TMPyP and ZnTMPyP in water.

The insertion of a metal causes a ref-shift over the Soret band. This is due to the changes in the energy levels decreasing the gap between HOMO-LUMO states indicating that the metal forms a stable square-planar complex with the porphyrin[15].

Emission Spectroscopy

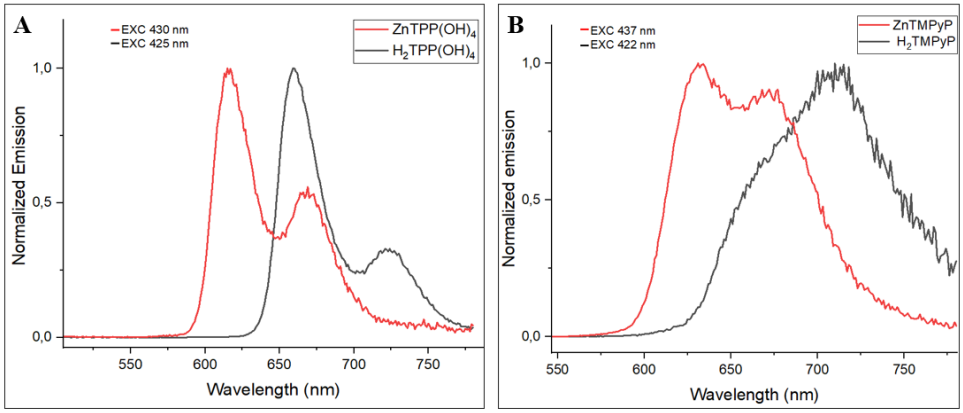

Figure 10 *A) Emission* spectra of *$H_2TPP(OH)_4$ and $ZnTPP(OH)_4$ in DMSO and B) Emission* spectra of *H_2TMPyP and ZnTMPyP in water.*

Figure 10 , displays emission spectra for porphyrins excited at their respective Soret bands. TPP porphyrins presented a blue shift of 45 nm and 55 nm for Q1 and Q2 respectively, from their free-core form to their metaled form. TMPyP from its free-core form to its metaled form had a blue shift of 40 nm concerning the emission band Q2. H_2TMPyP does not have well-defined Q bands, that can be wrongly interpreted as a single band. Some authors have reported that the 2 Q bands can be elucidated with the addition of ethanol[23]. The molar extinction coefficient of $ZnTPP(OH)_4$ and ZnTMPyP is 2.5 and 1.5 larger than for $H_2TPP(OH)_4$ and H_2TMPyP respectively, indicating the addition of metal improves its PL properties. Hydro-soluble porphyrin has a lower extinction coefficient. Authors[24] studied H_2TMPyP in different solvents, showing that porphyrin in water has the lowest absorption in comparison with other solvents such as DMSO or DMF. The statement aligns with our results.

Peripherical groups in meso positions determined the solubility of the porphyrin. Positively charged porphyrins are completely soluble in water while $H_2TPP(OH)_4$ and $ZnTPP(OH)_4$ are only soluble in organic solvents (ethanol, DMF, and DMSO).

The photophysical properties of the porphyrins and their metalated ones are summarized in **table 5**.

Porphyrin	$\lambda_{S\ (nm)}$	$\lambda_{Q\ (nm)}$	ε ($cm^{-1}\cdot M^{-1}$)	$\lambda_{emi\ (nm)}$
$H_2TPP(OH)_4$	425	Q1 :520 Q2 :560 Q3 :595 Q4 :652	330 245 ± 20587	660 725
$ZnTPP(OH)_4$	430	Q1:560 Q2:605	399 861 ± 5267	615 670
H_2TMPyP	422	Q1:520 Q2:560 Q3:585 Q4:635	117 087 ± 1342	710
ZnTMPyP	437	Q1:564 Q2:606	164525 ± 2676	630 672

Table 5. Summary of spectroscopical characterization of studied porphyrins. ($\lambda_{s\ (nm)}$ soret band, $\lambda_{Q\ (nm)}$ Q-bands, extinction coefficient: ε ($cm^{-1}\cdot M^{-1}$), and $\lambda_{emi\ (nm)}$ emission band.). Values were determined in DMSO for non-hydrosoluble porphyrine, and in water for hydrosoluble porphyrin.

4.3 Preliminary studies of GQDs and porphyrins

The formation of nanocomposites can be affected by several experimental parameters namely sonication time, temperature, and solvent. Mixing is an important parameter in the formation of nanocomposites. Sonication is used to disperse GQDs and porphyrins in the solvent, followed by agitation to improve the degree of mixing between acceptor and donor, to form π-π stacking. In literature, sonication time ranges from 15 minutes[17] up to 4 hours, with agitation times reaching 48 hours[25]. Previous studies were done here in the research group ICMMO, with longer times observing no formation of nanocomposites (1-hour sonication and 4 days stirring). Given this variability, the first experiment was conducted with 2 hours of sonication and measurements at room temperature. The effect of sonication on the intensity of the emission band of GQDs-EDA was studied. GQDs-EDA [0.016 mg/mL] in water were placed for 2 hours in sonication, and the emission spectrum was measured. No changes were observed. In terms of solvents, GQDs are soluble only in water while porphyrin $ZnTPP(OH)_4$ and $H_2TPP(OH)_4$ are non-hydro soluble. These porphyrins were solubilized in DMSO because it is an easily accessible water-miscible solvent. This choice made it necessary to conduct a series of experiments to determine the most suitable ratio of DMSO: H_2O to form assemblies of GQDs and non-hydrosoluble porphyrins.

4.3.1 Effect of the solvent in GQDs photophysical properties

A set of solutions was prepared with a gradual increase of DMSO keeping the concentration of GQDs constant [0.016 mg/mL] maintaining a constant volume of 3 mL. Then absorption and emission spectra were measured to assess changes in their photophysical properties. The results of the experiments are reported in **Figure 11.** Normalized absorption spectra show a red-shift as DMSO proportion increases. Such red-shift of the absorption band strongly depends on the solvent composition and is linked with an increase in particle sizes[12].

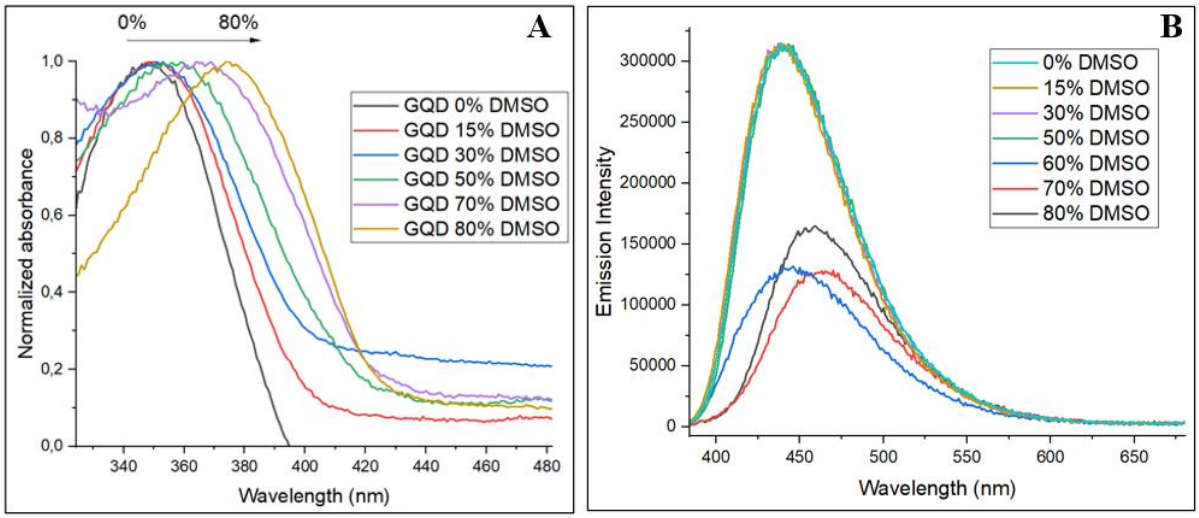

Figure 11 A) Normalized absorption spectra of GQDs-EDA [0,016 mg/mL] in water with consecutive additions of DMSO in a constant volume of 3 mL B) Emission spectra of GQDs-EDA in water with consecutive additions of DMSO.

The emission intensity of GQDs-EDAt has a significant quenching after 50% of DMSO. Additions up to 60% causes also a redshift over the emission band from 440 nm to 460 nm. A decrease in the intensity of emission is associated with precipitation or aggregation of GQDs.

4.3.2 Effect of the solvent in porphyrins photophysical properties

This study follows the previous one. The aim is to determine the highest water concentration that nanocomposites can withstand before aggregation or precipitation occurs.

In each experiment, 500 µL of a 9.0 x10^{-07} M porphyrin solution in DMSO was added in a constant volume of 3 mL. The water concentration was then increased from 20% to 80%. The 80% concentration was the highest percentage of water without affecting the overall concentration. A blue shift in absorption, due to solvatochromism, is observed after the addition of water. The absorption band starts to decrease after 50%. The absorbance of the Soret band at 85% water concentration is halved concerning the band at 100% DMSO (**Figure 12**). Some authors have found similar results but in the protonated form of $H_2TPP(OH)_4$ in ethanol after the addition of water.[16]

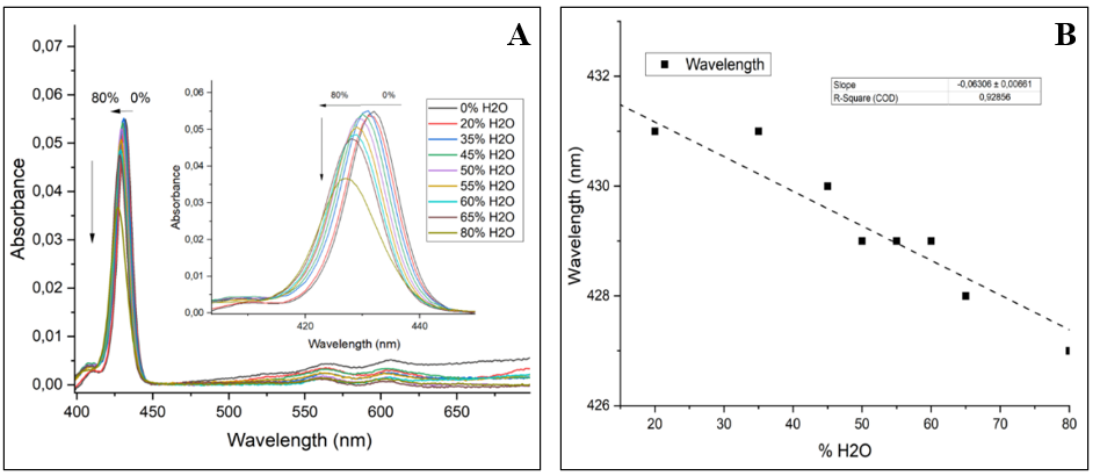

Figure 12 A) UV-VIS spectra of solution $ZnTPP(OH)_4$ [1.5E-07M] in DMSO with consecutive additions of water. B) Wavelength (nm) of Soret band vs percentage of water in solution.

The consecutive decrease in intensity of the Soret band after the addition of water is due to aggregation and precipitation of the porphyrin. At 80% of water, it is possible to see that the band decreases around 30% respecting the initial value with 100% DMSO.

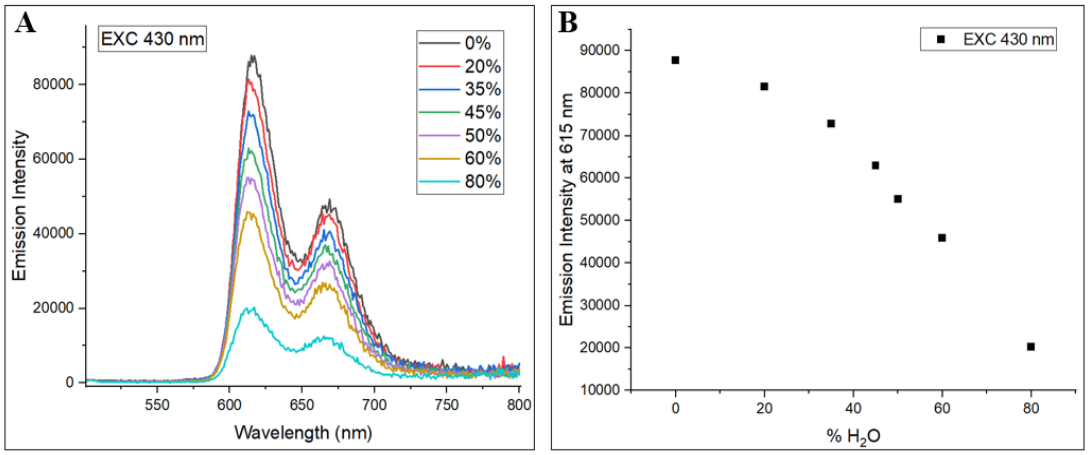

Figure 13 A) Emission spectrum of $ZnTPP(OH)_4$ in DMSO after consecutive additions of water B) Emission intensity at 615 nm (first Q-emission band) vs Percentage of water in solution.

The results of emission spectroscopy in **Figure 13** shows that water also causes a decrease in the emission band of porphyrins due to aggregation and precipitation. When water reaches 80% in volume the emission of fluorescence is largely quenched, dropping to about 25%. This experiment was repeated for $H_2TPP(OH)_4$, obtaining similar results. Both porphyrins show blue-shifted absorption bands in the presence of water.

In short, both porphyrin and GQDs are affected by solvent conditions. On the one hand, the addition of water up to 50% in volume leads to significant aggregation of porphyrin, as evidenced by a decrease of the Soret band followed by the quenching of fluorescence due to the change of porphyrin solution. On the other hand, the addition of DMSO up to 50% in volume causes a significant quenching of GQD emission. This is particularly intriguing because, in the literature, FRET studies often measure the donor's fluorescence emission without first evaluating the solvent's influence beforehand.

Based on the results of the two experiments, a 50:50 DMSO to H_2O ratio was determined to be optimal for subsequent studies.

4.4 Study of GQDs-Porphyrin assemblies

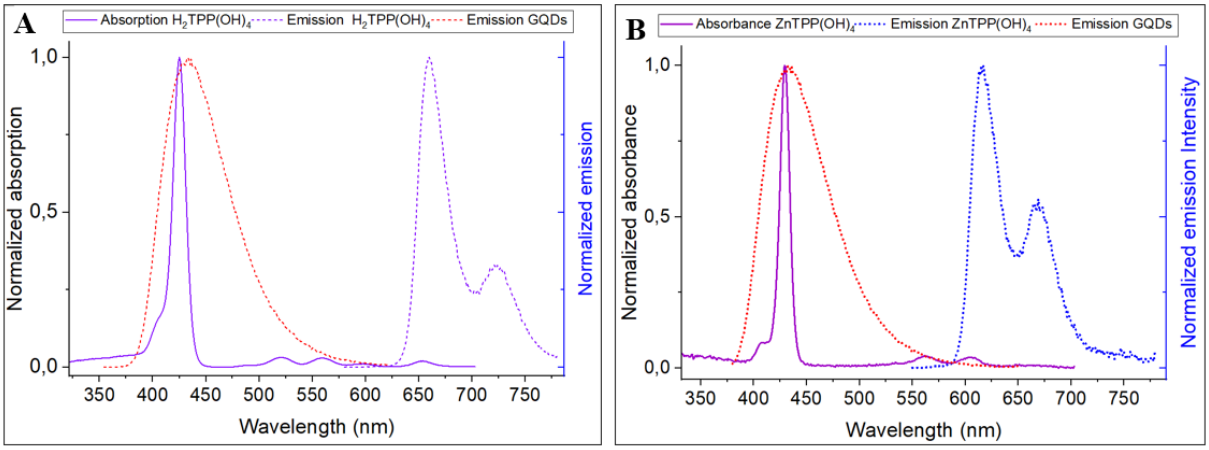

Figure 14. A) Normalized absorption spectrum of $H_2TPP(OH)_4$, normalized emission spectrum of GQDs-EDA in dashed red. Normalized emission spectrum of $H_2TPP(OH)_4$ when excited at 425 nm in dashed purple. B) Normalized absorption spectrum of $ZnTPP(OH)_4$, Normalized emission spectrum of GQDs with excitation at 350 nm, and normalized emission of $ZnTPP(OH)_4$, when excited at 430 nm

This experiment aimed to form assemblies between GQDs-EDA and four different porphyrins: $H_2TPP(OH)_4$, $ZnTPP(OH)_4$, H_2TMPyP, and ZnTMPyP, to study the effect on the photophysics of the element of the system Each of these systems, labeled as System **1**, **2**, **3**, and **4** respectively.

A set of solutions containing GQDs and porphyrins in different ratios (mmol of porphyrin/gram GQDs-EDA). Refer to *Chapter 3.2.4* for the preparation protocol. Steady-state emission spectroscopy was performed. Each sample's emission spectra were recorded by exciting the donor GQDs at their absorption band maxima (350 nm), allowing the detection of changes in the intensity of the donor's emission band without influencing the acceptor.

All experiments were conducted with donor and acceptor concentrations below 0.1 absorbance units (to avoid reabsorption artifacts also known as the inner filter effect). For each sample, a blank of porphyrin was prepared and throughout the whole experiment, they did not show any discernible band under excitation at 350 nm. In a previous study performed at ICMMO's laboratory, nanocomposites of ZnTPP and commercial GQDs were investigated, and the experiments revealed that reabsorption and inner filter effects happened at porphyrin concentrations exceeding 0.1 absorbance units. This resulted in attenuated emission intensity[13].

The shift of the Soret band position has been explained as the result of π-π interaction in similar D-A systems[17]. However, in our experiments, no shift in the Soret band position was observed and for that reason it was not included in the results section. This could lead to the conclusion that there is no π-π stacking. Let's investigate emission for each system.

Results of emission spectroscopy for system **1**: $H_2TPP(OH)_4$ and GQDs-EDA is presented in **Figure 15**. The experiment allowed us to detect a range of concentration in mmol of porphyrin per gram of GQDs-EDA where there is quenching, delimited in a purple box. Such quenching could be an indirect clue of porphyrin weak interaction with GQDs (Van der Waals interactions, since no π-π stacking was observed experimentally). Surprisingly the quenching is not clearly following the concentration of acceptor. At a higher concentration than $1.5x10^{-2}$ mmol/g, the initial signal of GQDs was recovered. A possible hypothesis is that at higher concentrations the interaction between porphyrin-porphyrin is more favorable than the interaction between porphyrin-GQDs. We prepared again the experiments in the range of concentration from $2.3x10^{-03}$ to $1.1x10^{-02}$ mmol of $H_2TPP(OH)_4$ and quenching is again observed without any clear trend as a function of concentration). A similar behavior was observed in $ZnTPP(OH)_4$, observing quenching with diluted concentration of porphyrin and recovery of donor emission at higher porphyrin concentration. The summary of results is reported in **Table *6***.

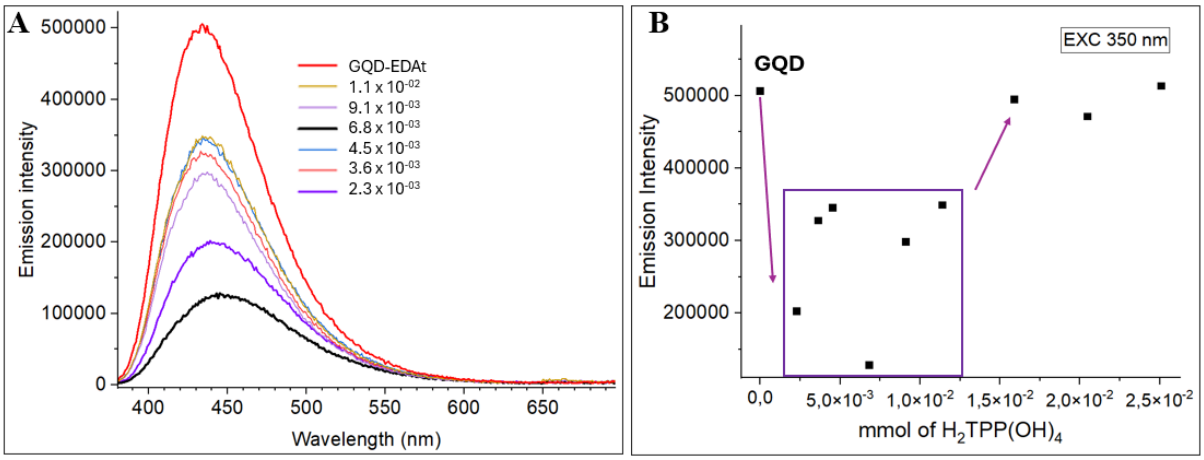

Figure 15 A) Emission spectra for nanocomposites of $H_2TPP(OH)_4$ and GQDs-EDA. B) Plot emission intensity at 440 nm vs mmol of $H_2TPP(OH)_4$ per gram of GQDs-EDA

composite	Presence of Quenching	Range mmol of porphyrin/ g of GQDs-EDA	Maximum quenching	composite mmol TPP/g GQDs
GQDs/$H_2TPP(OH)_4$	Yes	$2.0x10^{-3}$ - $1.5x10^{-2}$	80%	$7x10^{-3}$
GQDs/$ZnTPP(OH)_4$	Yes	$6.7x10^{-3}$ - $1.1x10^{-2}$	55%	$9x10^{-3}$

Table 6. The range of concentration in mmol of porphyrin per gram of GQDs, whet it is observed quenching. The maximum value of quenching observed and its respective concentration.

The experiments made of GQDs-EDA as donors and $H_2TPP(OH)_4$ and $ZnTPP(OH)_4$ as acceptors, and under the proposed conditions of solvent, sonication, and agitation showed that there is a ratio mmol of porphyrin/g of GQDs-EDA where quenching can be observed. The absence of the emission band of the acceptor, in all the experiments, makes us conclude the absence of FRET. At least the sensitization of porphyrin by GQDs could not be measured with the available fluorimeter (signal/radio noise).

As a proposal to the non-linear dependance of quenching, a higher time of agitation can be used to observe if the trend can be observed. Sonication is to guarantee the dispersion of the molecules, longer times could lead to degradation of any part involved in the system, but a mild agitation could improve the interaction between donor and acceptor.

For hydrosoluble porphyrins, the same protocol was followed as before. For **system 3**, made of H_2TMPyP and GQDs-EDA, no changes in their emission band were observed at any addition of porphyrin. The absence of quenching could indicate that there is no interaction between porphyrin and GQDs-EDA which leads to no formation of nanocomposites. This is somehow surprising since GQDs are negatively charged whereas H_2TMPyP is positively charged.

For **system 4**, between ZnTMPyP and GQDs-EDA, a decrease in the emission occurs and is dependent on the concentration of porphyrin. The emission spectra are reported in ***Figure 16***.

GQDs emission band is quenched after the addition of porphyrin, but there is no increase of the acceptor's band. Data was analyzed through the Stern-Volmer equation (Equation 1) to study the nature of the quenching.

$$\frac{I_O(GQDs)}{I(Composites)} = 1 + K_{sv}[ZnTMPyP] \qquad \text{Eq 1}$$

Where I_0 and I, correspond to emission intensity of quantum dots without porphyrin and in the nanocomposites respectively, at excitation of 350 nm, Ksv as the quencher rate coefficient and $[ZnTMPyP]$ as the concentration of porphyrin added.

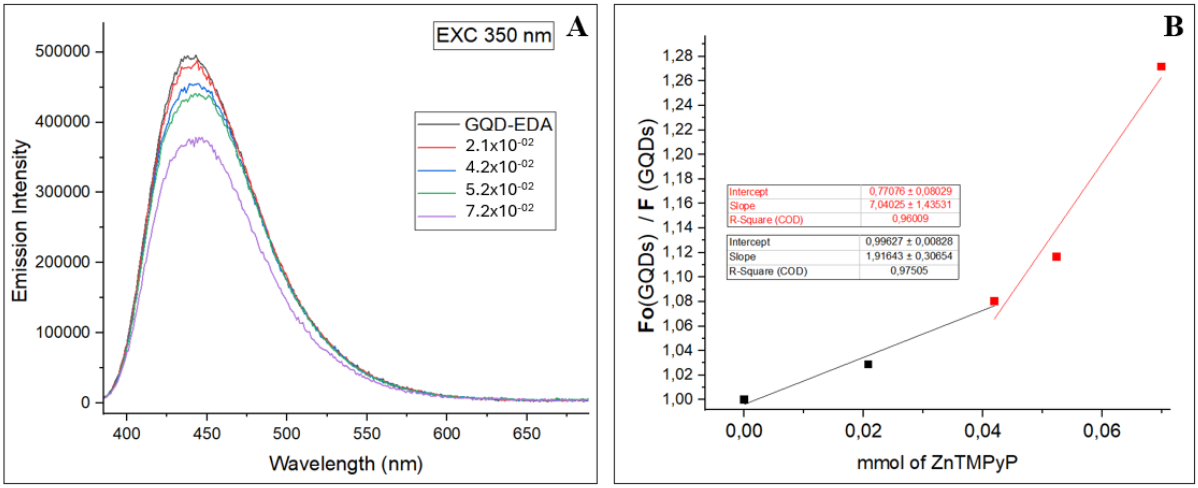

Figure 16 A) Emission spectra of nanocomposites of ZnTMPyP and GQDs-EDA. B) Stern-Volmer linearization for quenching analysis.

The results are graphed in **Figure 16 B**). The trend has two slopes indicating two quenching slopes Ksv of 1.91 and 7.04 in g/mol. This could be correlated to a combination of dynamic and static quenching.[26] In dynamic quenching excited state of the fluorophore interacts (GQDs in excited state : GQDs*) with the quencher resulting in a deactivation of GQDs to the ground state. Given that dynamic quenching is related to a diffusion dependence process, it could be a confirmation of the interaction between GQDs* and porphyrin (collision mechanism). Static quenching occurs when the molecules in contact create a complex in the ground state before excitation.[13]

The observation of two quenching modes could also suggest the presence of aggregates. Authors have reported that sonication can affect the concentration of porphyrin in solution by the formation of aggregates[27]. In addition, TMPyP tends to aggregate more in aqueous media than in organic solvents as was reported in other studies[24]. Monomers and aggregates could interact and quench the GQDs by different mechanisms, at low concentrations “monomers” of ZnTMPyP quenches GQDs, at higher concentration dimers or ZnTMPyP aggregates become the quenchers. The mechanim of quenching is not yet elucidated.

The positive character of this porphyrin as well as the metalation could bring stability to the interaction between GQDs and porphyrin. The observed quenching is an indirect proof of the formation (even in a transient mode) of a nano-assemblie between GQDs and ZnTMPyP. As FRET was not observed in this system, we could suggest that other energy transfer processes could be occurring therefore causing quenching. The mechanim of quenching is yet not elucidated (due to lack of time for this study).

Quenching is due to a variety of molecular interactions as excited-state reactions, molecular rearrangements, energy transfer, ground-state complex formation, and collisional quenching. Aside from resonance energy transfer, quenching can be through electron exchange and photoinduced electron transfer. Quenching can occur also by a combination of these mechanisms.[13] This indicates, that it is necessary to study this possible mechanism that could be happening instead of FRET. Authors have found electron transfer between porphyrin and GQDs[28]. This approach could be interesting to study because they studied GQDs as electron acceptors and porphyrins as electron donors, favored by the values of their LUMO and HOMO

energy levels. They report a LUMO for GQDs of -3.58 eV while -2.78 eV for the porphyrin (H_2TPP). This could explain why there is no presence of FRET in any of the proposed systems donor-acceptor.

5 Conclusions

In this work, GQDs doped with nitrogen atoms with EDA were synthesized using a hydrothermal approach and characterized through DLS, Z-Potential, Luminescence quantum yield, absorption and emission spectroscopy, and FT-IR. The nanoparticles presented a hydrodynamic diameter of 0.83 nm, a luminescence quantum yield of 47%, an absorption band at 346 nm in water redshifted after the addition of DMSO, an emission band at 440 nm when excited at 350 nm with a functional group in their surface such as -COOH -OH and -NH observed through FT-IR. They presented stability over time and homogeneity when excited at different wavelengths between 340 and 380 nm. The effect of solvent was studied by observing a redshift after the addition of DMSO in water, and a decrease of emission intensity after 50% addition of H_2O.

Porphyrin $ZnTPP(OH)_4$ was successfully synthesized using $H_2TP(OH)_4$ as a precursor using a one-pot reaction that was confirmed through NMR, absorption, and emission spectroscopy. Porphyrins $H_2TPP(OH)_4$, H_2TMPyP, and ZnTMPyP were characterized through absorption and emission spectroscopy, and the solvent effect was studied on $H_2TPP(OH)_4$ and $ZnTPP(OH)_4$ on DMSO observing a blue shift when water is added, and significant aggregation after 50% addition of water.

Synthetized GQDs-EDA and porphyrins were used to study the formation of nanocomposites and their photophysics. Results suggest that under the proposed conditions there is no presence of FRET between any of the studied porphyrins.

With $H_2TPP(OH)_4$ quenching is observed when solutions are formed in the range of concentration between $2.0x10^{-3}$ - $1.5x10^{-2}$ mmol of porphyrin per gram of GQDs-EDA, observing an 80% maximum of quenching at the concentration $7x10^{-3}$ mmol/g. For $ZnTPP(OH)_4$, the range was found between $6.7x10^{-3}$ - $1.1x10^{-2}$ mmol/g and 55% maximum of quenching at $9x10^{-3}$. In solutions made of ZnTMPyP linear quenching was observed (with a 2-regime mode). For H_2TMPyP no quenching was observed indicating that the metalation can affect positively the quenching.

The presence of quenching suggests that GQDs and porphyrin could interact and be assembled. The nature of the interaction is not yet well-understood (we were expecting π-π interaction, but no redshift on Soret band was observed). FRET was not demonstrated, as we can observe the quenching of the luminescence of the donor, but we could not observe the emission of the acceptor (sensitization). The presence of other transfer processes should be studied to determine if the D-A couples can be suitable for future use as a detection method in biosensors.

6 Future perspectives

This study included a preliminary study of the formation of nanocomposites using several porphyrins and commercial GQDs, that allowed us to understand the conditions in terms of concentration of porphyrin and their influence in the interpretation of the data. This new approach allowed the possibility of the presence of other energy transfer phenomena than the expected FRET. In addition, this report underlines the importance of studying the influence of

time of sonication, agitation, and solvent on each of the parts involved in the donor-acceptor couple.

A second approach is the study of an electron transfer process to explain the absence of FRET and give space to propose a new donor-acceptor couple. This study can be done with ZnTMPyP for its solubility in water and the presence of quenching. This study will include excitation spectroscopy of the samples and TCSPC to track the changes in donors' lifetime. Characterization of acceptor and donor should be done, including redox potentials and quantum yields.

The formation of a suitable donor-acceptor couple is open to many possibilities that include the study of multiple variables, to find the most appropriate conditions.

7 Bibliography

(1) Kaur, B.; Kumar, S.; Kaushik, B. K. Trends, Challenges, and Advances in Optical Sensing for Pathogenic Bacteria Detection (PathoBactD). *Biosensors and Bioelectronics: X* **2023**, *14*, 100352. https://doi.org/10.1016/j.biosx.2023.100352.

(2) Singh, A. K.; Mittal, S.; Das, M.; Saharia, A.; Tiwari, M. Optical Biosensors: A Decade in Review. *Alexandria Engineering Journal* **2023**, *67*, 673–691. https://doi.org/10.1016/j.aej.2022.12.040.

(3) Reja, S. I.; Minoshima, M.; Hori, Y.; Kikuchi, K. Recent Advancements of Fluorescent Biosensors Using Semisynthetic Probes. *Biosensors and Bioelectronics* **2024**, *247*, 115862. https://doi.org/10.1016/j.bios.2023.115862.

(4) Paul, R.; Suklabaidya, S.; Arshad Hussain, S. Fluorescence Resonance Energy Transfer (FRET) as Biomarkers. *Materials Today: Proceedings* **2021**, *46*, 6301–6303. https://doi.org/10.1016/j.matpr.2020.05.217.

(5) Anton, S. Charakterisierung Der Rezeptor-Assoziierten cAMP Nanodomänen Des Humanen Glucagon-like Peptide 1 Rezeptors Mittels FRET-Basierter Sensoren. **2019**.

(6) Verma, A. K.; Noumani, A.; Yadav, A. K.; Solanki, P. R. FRET Based Biosensor: Principle Applications Recent Advances and Challenges. *Diagnostics* **2023**, *13* (8), 1375. https://doi.org/10.3390/diagnostics13081375.

(7) Liu, Y.; Hu, X.; Liang, F.; Cao, Y. A FRET Sensor Based on Quantum Dots–Porphyrin Assembly for Fe(III) Detection with Ultra-Sensitivity and Accuracy. *Anal Bioanal Chem* **2022**, *414* (26), 7741–7751. https://doi.org/10.1007/s00216-022-04305-y.

(8) Naik, M. J. P.; Mohanta, S.; Mandal, P.; Saha, M. N-Doped Graphene Quantum Dots Using Different Bases. *Int. J. Nanosci.* **2019**, *18* (01), 1850017. https://doi.org/10.1142/S0219581X18500175.

(9) Son, D.; Choi, W. New Nanoscale Material: Graphene Quantum Dots. In *Nanomaterials, Polymers, and Devices*; Kong, E. S. W., Ed.; Wiley, 2015; pp 141–194. https://doi.org/10.1002/9781118867204.ch6.

(10) Kumar, Y. R.; Deshmukh, K.; Sadasivuni, K. K.; Pasha, S. K. K. Graphene Quantum Dot Based Materials for Sensing, Bio-Imaging and Energy Storage Applications: A Review. *RSC Adv.* **2020**, *10* (40), 23861–23898. https://doi.org/10.1039/D0RA03938A.

(11) Wang, L.; Zhu, S.; Wang, H.; Wang, Y.; Hao, Y.; Zhang, J.; Chen, Q.; Zhang, Y.; Han, W.; Yang, B.; Sun, H. Unraveling Bright Molecule-Like State and Dark Intrinsic State in

Green-Fluorescence Graphene Quantum Dots via Ultrafast Spectroscopy. *Advanced Optical Materials* **2013**, *1* (3), 264–271. https://doi.org/10.1002/adom.201200020.

(12) Cui, L.; Ren, X.; Sun, M.; Liu, H.; Xia, L. Carbon Dots: Synthesis, Properties and Applications. *Nanomaterials* **2021**, *11* (12), 3419. https://doi.org/10.3390/nano11123419.

(13) Lakowicz, J. R. *Principles of Fluorescence Spectroscopy*, 3rd ed.; Springer: New York, 2006.

(14) Taniguchi, M.; Lindsey, J. S.; Bocian, D. F.; Holten, D. Comprehensive Review of Photophysical Parameters (ε, Φf, Ts) of Tetraphenylporphyrin (H2TPP) and Zinc Tetraphenylporphyrin (ZnTPP) – Critical Benchmark Molecules in Photochemistry and Photosynthesis. *Journal of Photochemistry and Photobiology C: Photochemistry Reviews* **2021**, *46*, 100401. https://doi.org/10.1016/j.jphotochemrev.2020.100401.

(15) Giovannetti, R. The Use of Spectrophotometry UV-Vis for the Study of Porphyrins. In *Macro To Nano Spectroscopy*; Uddin, J., Ed.; InTech, 2012. https://doi.org/10.5772/38797.

(16) Zannotti, M.; Giovannetti, R.; Minofar, B.; Řeha, D.; Plačková, L.; D'Amato, C. A.; Rommozzi, E.; Dudko, H. V.; Kari, N.; Minicucci, M. Aggregation and Metal-Complexation Behaviour of THPP Porphyrin in Ethanol/Water Solutions as Function of pH. *Spectrochimica Acta Part A: Molecular and Biomolecular Spectroscopy* **2018**, *193*, 235–248. https://doi.org/10.1016/j.saa.2017.12.021.

(17) Gao, X.; Zhang, B.; Zhang, Q.; Tang, Y.; Liu, X.; Li, J. The Influence of Combination Mode on the Structure and Properties of Graphene Quantum Dot-Porphyrin Composites. *Colloids and Surfaces B: Biointerfaces* **2018**, *172*, 207–212. https://doi.org/10.1016/j.colsurfb.2018.08.010.

(18) Xue, G.; Yu, S.; Qiang, Z.; Xiuying, L.; Tang Lijun; Jiangrong, L. Application of Maleimide Modified Graphene Quantum Dots and Porphyrin Fluorescence Resonance Energy Transfer in the Design of '"Turn-on"' Fluorescence Sensors for Biothiols. *Analytica Chimica Acta* **2020**, *1108*, 46–53. https://doi.org/10.1016/j.aca.2020.01.062.

(19) Lewandowska-Andralojc, A.; Gacka, E.; Pedzinski, T.; Burdzinski, G.; Lindner, A.; O'Brien, J. M.; Senge, M. O.; Siklitskaya, A.; Kubas, A.; Marciniak, B.; Walkowiak-Kulikowska, J. Understanding Structure–Properties Relationships of Porphyrin Linked to Graphene Oxide through π–π-Stacking or Covalent Amide Bonds. *Sci Rep* **2022**, *12* (1), 13420. https://doi.org/10.1038/s41598-022-16931-8.

(20) Qu, D.; Zheng, M.; Zhang, L.; Zhao, H.; Xie, Z.; Jing, X.; Haddad, R. E.; Fan, H.; Sun, Z. Formation Mechanism and Optimization of Highly Luminescent N-Doped Graphene Quantum Dots. *Sci Rep* **2014**, *4* (1), 5294. https://doi.org/10.1038/srep05294.

(21) Zhu, S.; Bai, X.; Wang, T.; Shi, Q.; Zhu, J.; Wang, B. One-Step Synthesis of Fluorescent Graphene Quantum Dots as an Effective Fluorescence Probe for Vanillin Detection. *RSC Adv.* **2021**, *11* (16), 9121–9129. https://doi.org/10.1039/D0RA10825A.

(22) Kalluri, A.; Dharmadhikari, B.; Debnath, D.; Patra, P.; Kumar, C. V. Advances in Structural Modifications and Properties of Graphene Quantum Dots for Biomedical Applications. *ACS Omega* **2023**, *8* (24), 21358–21376. https://doi.org/10.1021/acsomega.2c08183.

(23) Habib, M. A.; Sarker, A. K.; Tabata, M. Interactions of DNA with H2TMPyP4+and Ru(II)TMPyP4+: Probable Lead Compounds for African Sleeping Sickness. *Bangla Pharma J* **2015**, *17* (1), 79–85. https://doi.org/10.3329/bpj.v17i1.22321.

(24) Sallam, G.; Shaban, S. Y.; Nassar, A.; El-Khouly, M. E. Water Soluble Porphyrin as Optical Sensor for the Toxic Heavy Metal Ions in an Aqueous Medium. *Spectrochimica Acta Part A: Molecular and Biomolecular Spectroscopy* **2020**, *241*, 118609. https://doi.org/10.1016/j.saa.2020.118609.

(25) Achadu, O. J.; Uddin, I.; Nyokong, T. Fluorescence Behavior of Nanoconjugates of Graphene Quantum Dots and Zinc Phthalocyanines. *Journal of Photochemistry and Photobiology A: Chemistry* **2016**, *317*, 12–25. https://doi.org/10.1016/j.jphotochem.2015.11.006.

(26) Singh, V. K.; Mishra, H.; Ali, R.; Umrao, S.; Srivastava, R.; Abraham, S.; Misra, A.; Singh, V. N.; Mishra, H.; Tiwari, R. S.; Srivastava, A. In Situ Functionalized Fluorescent WS_2 -QDs as Sensitive and Selective Probe for Fe^{3+} and a Detailed Study of Its Fluorescence Quenching. *ACS Appl. Nano Mater.* **2019**, *2* (1), 566–576. https://doi.org/10.1021/acsanm.8b02162.

(27) Nomura, H.; Koda, S.; Yasuda, K.; Kojima, Y. Quantification of Ultrasonic Intensity Based on the Decomposition Reaction of Porphyrin. *Ultrasonics Sonochemistry* **1996**, *3* (3), S153–S156. https://doi.org/10.1016/S1350-4177(96)00020-X.

(28) Pallikkara, A.; Sebastian, D.; Ramakrishnan, K. An Investigation on the Effect of Extended Conjugation on the Photophysical Properties of Graphene Quantum Dot-Porphyrin Dyads. *ChemistrySelect* **2021**, *6* (43), 12224–12232. https://doi.org/10.1002/slct.202103199.

(29) G. Singh, S. Chandra, *Electrochem Sci Adv*. 2023, 3, e2100149. https://doi.org/10.1002/elsa.202100149

(30) Riya Sinha, Odhavia Sahil Jaykishan, and Pradipta Purkayastha Langmuir 2023 39 (31), 11108-11118
DOI: https://doi.org/10.1021/acs.langmuir.3c01466